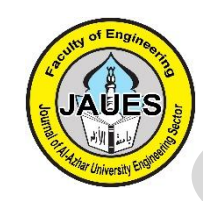


# Journal of Al-Azhar University Engineering Sector



Vol. 20, No. 77, October 2025, 1174-1187

# BUILDING'S VULNERABILITY ASSESSMENT TO FLOOD HAZARDS ON EGYPT'S MEDITERRANEAN COAST USING REMOTE SENSING AND AHP

Mohamed Hisham<sup>1\*</sup>, Mohamed T. Elnabwy<sup>2</sup>, Emad Elbeltagi<sup>1</sup>, Ibrahim Motawa<sup>1</sup>

<sup>1</sup>Structural Engineering Department, Faculty of Engineering, Mansoura University, Mansoura 35516, Egypt.

<sup>2</sup>Coastal Research Institute (CORI), National Water Research Center, Alexandria 21415, Egypt.

\* Correspondence: mohamdhishamm@std.mans.edu.eg

#### Citation:

M. Hisham, M. T. Elnabwy, E. Elbeltagi, I. Motawa. "Building's vulnerability assessment to flood hazards on egypt's mediterranean coast using remote sensing and AHP", Journal of AlAzharUniversity Engineering Sector, vol. 20 (77), pp. 1174-1187, 2025.

Received: xx May 20xx
Revised: xx May 20xx
Accepted: xx August 20xx

Doi:

Copyright © 2025 by the authors. This article is an open access article distributed under the terms and conditions Creative Commons Attribution-Share Alike 4.0 International Public License (CC BY-SA 4.0)

#### **ABSTRACT**

This study systematically identifies critical flood determinants in Egypt's Nile Delta, focusing on the impacts of Mediterranean Sea-level rise (SLR). Using an integrated RS-GIS approach with Google Earth Engine (GEE) cloud computing, we analyze Landsat 8 imagery and SRTM DEM data to derive six key risk parameters: elevation (EI), slope (SI), land use (LU), vegetation index (VI), water index (WI), and soil permeability infiltration level (SPIL). These indices were normalized in ArcMap for enhanced visualization, and the Analytic Hierarchy Process (AHP) was applied to weight flood hazard indices and generate a spatial risk assessment. Results reveal that the northwestern Nile Delta, particularly Kafr El-Sheikh Governorate along the eastern flank of the Rosetta Nile branch near Burullus Lake, faces the highest flood exposure. This vulnerable coastal zone spans 40 km linear and lies between the Mediterranean shoreline and Lake El-Burullus, encompassing approximately 11,000 buildings at risk of static flooding. The GIS-AHP-based flood hazard mapping highlights high-risk zones, providing critical insights for targeted flood risk management and protective measures in the region.

**KEYWORDS**: Remote Sensing, Static Flood, Google Earth Engine, AHP, Flood Risk Mapping.

# المباني للتأثر بمخاطر الفيضانات في سواحل البحر الأبيض المتوسط في مصر باستخدام الاستشعار عن تقييم قابلية بعد وعملية التسلسل الهرمي التحليلي

محمد هشام'\*، محمد تروت النبوي'، عماد البلتاجي'، إبراهيم مطاوع'

ا قسم الهندسة الإنشائية، كلية الهندسة، جامعة المنصورة، المنصورة ٢١٥٥٦، مصر. ٢ معهد بحوث الشواطئ، المركز القومي لبحوث المياة، الإسكندرية ٥١٤١، مصر. البريد الاكتروني للباحث الرئيسي: mohamdhishamm@std.mans.edu.eq

#### الملخص

تحدد هذه الدراسة بشكل منهجي محددات الفيضانات الحرجة في دلتا النيل في مصر، مع التركيز على آثار ارتفاع مستوى سطح البحر في البحر الأبيض المتوسط. باستخدام نهج الاستشعار عن بعد وأنظمة المعلومات الجغرافية المتكامل مع الحوسبة السحابية Engine Earth Google (GEE) ، قمنا بتحليل صور لاند سات ٨ وبيانات نموذج الارتفاع الرقمي لمهمة تضاريس الرادار المكوكية لاشتقاق ستة معاملات رئيسية للخطر: الارتفاع والمنحدر واستخدام الأراضي ومؤشر الغطاء النباتي ومؤشر المياه ومستوى تسلل نفاذية التربة. تم تطبيع هذه المؤشرات في ArcMap لتعزيز التصور، وتم تطبيق عملية التسلسل الهرمي التحليلي على وزن مؤشرات مخاطر الفيضانات وإنشاء تقييم للمخاطر المكانية. وتكشف النتائج أن دلتا النيل الشمالية الغربية، وخاصة محافظة كفر الشيخ على طول الجهة الشرقية لفرع نهر رشيد بالقرب من بحيرة برلس، تواجه أعلى نسبة تعرض للفيضانات. تمتد هذه المنطقة الساحلية المعرضة للخطر لحوالي ٤٠ كم طولي والتي تقع بين ساحل البحر الأبيض المتوسط وبحيرة البرلس ، وتضم ما يقرب من ١١٩٠٠ مبنى معرضة لخطر الفيضانات المستهدفة وتدابير الحماية في المناطق عالية الخطورة ، مما يوفر رؤى مهمة لإدارة مخاطر الفيضانات المستهدفة وتدابير الحماية في المناطق.

الكلمات المفتاحية: الاستشعار عن بعد، الفيضانات الساكنة، محرك جوجل إرث، عملية التسلسل الهرمي التحليلي، رسم خرائط مخاطر الفيضانات.

# 1. INTRODUCTION

As global warming progresses, one immediate consequence within the climate system is the in sea level rise (SLR), often referred to as static flooding. This sea level increase results from thermal expansion of ocean waters and meltwater contributions from continental ice sheets and mountain glaciers. Floods stand out as among the most devastating and lethal natural calamities. Annually, millions of individuals worldwide face the impacts of flooding, resulting in substantial economic losses averaging around \$50 billion. [1,2]. Recent decades have witnessed a marked increase in global flood frequency, resulting in substantial economic losses from both direct infrastructure damage and indirect socioeconomic disruptions. This trend will continue due to population growth, urbanization, deteriorating infrastructure, and climate change impacts [3]. Rising sea levels and heavy rainfall, influenced by climate change and land subsidence, contribute to coastal flooding [4]. The IPCC's Sixth Assessment Report highlights the worsening effects of climate change on natural systems and predicts increased coastal flood risks worldwide. The report forecasts a potential SLR of 0.40 to 0.84 meters by 2081-2100, with an estimated rate of change of 3.4 mm/year (± 0.4) [4].

Flooding ranks among the most prevalent and devastating natural hazards globally, impacting nations across all continents [5,6]. Major flood categories include: (i) rapidly occurring flash floods that reduce in frequency progressively, pluvial floods stemming from precipitation exceeding urban drainage capacity, and fluvial floods originating from river systems. [1,3,7–9]. (ii) static flooding, which increases in frequency over time and occurs gradually, like SLR [3,10,11]. The extensive flooding of coastal lowlands and subsequent impacts on built environments and infrastructure systems are direct consequences of SLR. The rising water levels induced by SLR progressively exacerbate land subsidence, leading to cumulative structural damage to infrastructure and buildings over extended periods [12].

Numerous studies have investigated diverse methodologies to assess the effects of sealevel rise (SLR) on coastal zones. While some research has examined SLR impacts at a global scale [13–18], the majority of studies focus on regional or localized geographical areas. This disparity may arise from the inherent complexities of large-scale analyses, including challenges associated with extensive datasets, spatial variability in coastal dynamics, and limitations in data availability and resolution.

Numerous studies have investigated the effects of SLR on coastal regions at a regional scale. For instance, [19] assessed SLR and storm surge consequences in the Fiji Islands, while [20] evaluated climate change impacts on the Nile Delta's coastal zone. Similarly, [21] studied SLR effects in the Kingdom of Bahrain, and [22] analyzed potential SLR impacts along the coastal zone of Kanyakumari District, Tamil Nadu, India. Additionally, [23] examined coastal inundation vulnerability due to SLR in Semarang City, Indonesia, and [24] conducted a city-based SLR assessment for the Turkish Coastal Zone.

Egypt's Nile Delta is a critical case study for climate change impacts on low-lying coastal regions. According to IPCC AR5 findings, the Mediterranean coastline of the Nile Delta exhibits particular susceptibility to SLR. Instrumental records from tide gauges indicate an annual SLR rate of 2.2 mm in the delta's eastern sector [25]. Occupying merely 2% of Egypt's total territory, the Nile Delta sustains 41% of the national population and contains vital economic infrastructure, including energy facilities and coastal tourism developments [26]. This confluence of factors, dense population, low-lying geography, SLR threats, and increased flooding, renders the Delta highly vulnerable. Analysis of satellite imagery and GIS data reveals that a 50 cm SLR could displace more than two million residents in these cities, potentially losing 214,000 jobs and over \$35 billion in land value, property assets, and tourism revenue[27]. The irreversible damage to globally significant historical, cultural, and archaeological heritage remains incalculable. Further research is needed to evaluate the risks faced by other low-lying regions in Egypt beyond these urban areas.

The challenges presented by the lack of a standardized disaster prevention system further exacerbate the vulnerability of coastal communities, underscoring the need for a robust Pre-Disaster Management Framework. This study proposes an integrated pre-disaster management framework for coastal buildings to address these challenges and promote long-term sustainability. This framework will employ advanced methodologies, incorporating sophisticated geospatial tools, numerical modeling, and artificial intelligence (AI) approaches. The primary objective of this investigation is to analyze and evaluate the impacts of SLR on the Nile Delta region in Egypt. This will be achieved through a comprehensive framework that prioritizes the understanding of environmental processes to assess the susceptibility of coastal communities to SLR. The research will explore the application of GIS methods in modeling SLR scenarios, focusing on the data and processing requirements necessary for accurate impact assessments. Additionally, a GIS simulation model will be developed to evaluate the potential effects of an SLR ranging from zero to one meter on the coastal zones of the Nile Delta. Overall, this study utilizes geographic information systems (GIS) and geospatial analytical techniques to investigate the implications of SLR on the coastal regions of the Nile Delta.

The manuscript is organized systematically: Section **Error! Reference source not found.** describes the integrated GIS-AHP methodological framework for building evaluation; Section 3 presents and analyzes the results, while Sections 0 provide concluding remarks and policy recommendations, respectively.

#### 2. METHODOLOGY

#### 2.1. Study Area

Egypt contains the Nile Valley and Delta system - the planet's largest river-fed oasis formed by the world's longest river system, occupying approximately 1 million km² in northeast Africa. This geomorphological feature, situated at the Nile-Mediterranean confluence in northern Egypt, ranks among Earth's most expansive deltas [28]. It's a triangular-shaped region formed by the deposition of fertile soil carried by the Nile over millennia. The Nile Delta is located between longitudes 30° 22′ 00″ E and 31° 50′ 00″ E and latitudes 31° 36′ 00″ N and 30° 12′ 00″ N [29]. Demographic data reveals the Nile Delta's disproportionate population density, containing 41% of Egypt's residents within just 2% of its territory [30], [31]. As one of the world's most densely populated deltaic systems, it experiences competing hydrological stresses from northern coastal processes and southern riverine flows [26,32]. Moreover, the Delta is a nexus of critical infrastructures and buildings that underpin Egypt's economy and society. Its strategic location has led to the development of major transportation networks, including highways, railways, and waterways, facilitating trade and commerce both domestically and internationally. Furthermore, the Nile Delta comprises eleven governorates, namely Qalyobia, Gharbia, Monofiya, Sharkia, Port Said, Ismailia, Dakahliea, Damietta, Kafr El-Sheikh, El-Bohaira, and Alexandria[33], as illustrated in Fig. 1.

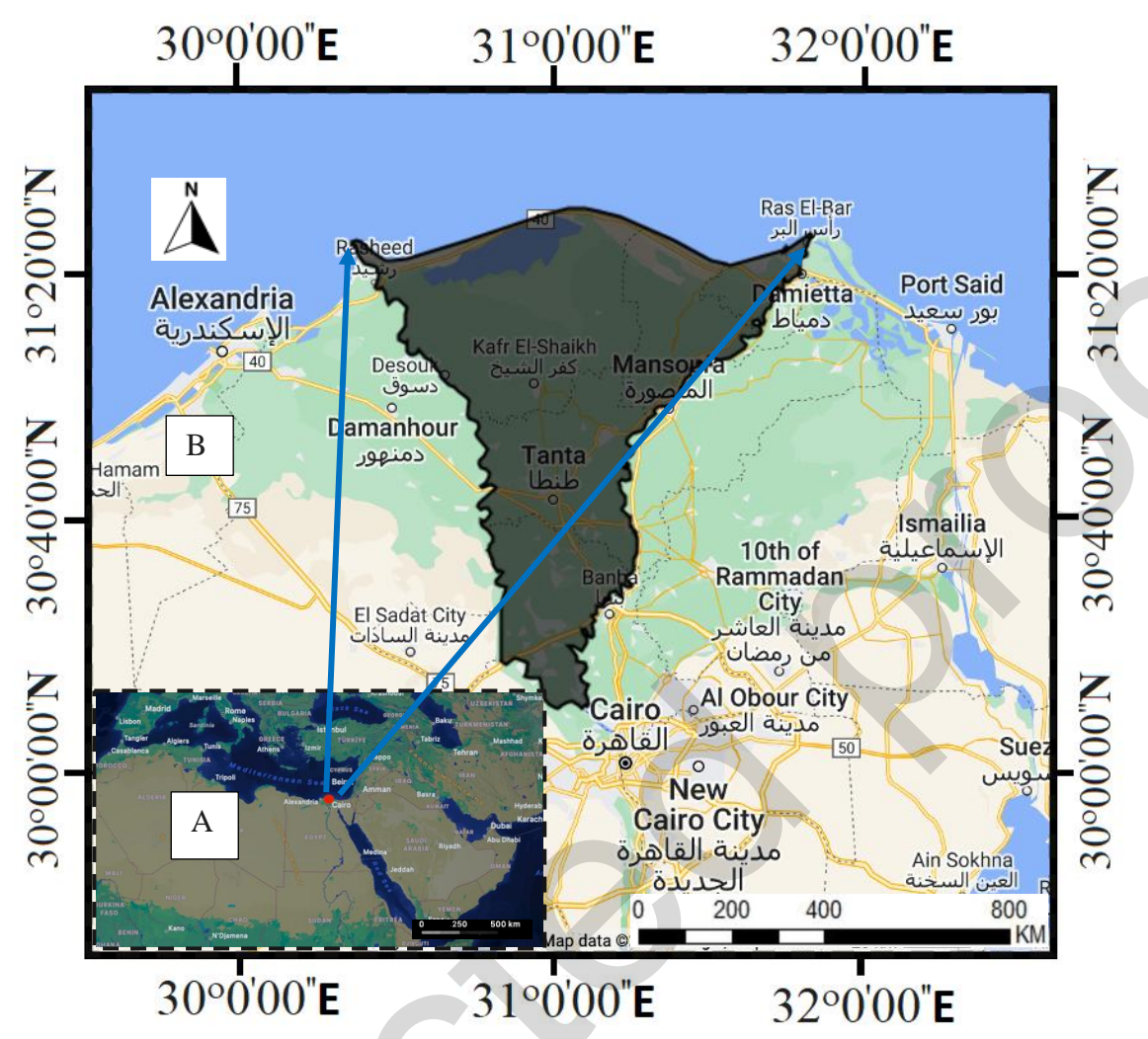


**Fig. 1.** The location of this study is shown by the red dot in (A) and the study area boundary line in (B).

Consequently, SLR associated with climate change presents substantial risks to Egypt's Nile Delta, threatening built environments, ecological systems, and populated areas [34]. Additionally, land subsidence, water and natural gas extraction, and other critical natural aspects heighten vulnerability to coastal flooding and reduce freshwater supply to the delta [35]. IPCC projections indicate approximately 2,660 square kilometers of the northern Nile Delta face permanent inundation by 2100 [25,36].

This study focuses on the Nile Delta region due to three key geographical characteristics: (I) its low-lying topography resulting from millennia of fluvial sedimentation, (II) an extensive 150+ km Mediterranean coastline vulnerable to marine processes, and (III) dense urbanization including major population centers like Alexandria, Port Said, Rosetta, and Damietta.

#### 2.2. Materials and Methods

A computational framework, in this context, refers to a structured environment that combines various software tools and methodologies to solve qualitative and quantitative approaches to exposure modeling with spatial analysis. Here's a breakdown of the tools and how they might fit within the framework:

#### **GEE and Data Sources**

This study employed Google Earth Engine (GEE), a cloud-based geospatial analysis platform, for computational workflows. GEE facilitates large-scale processing of Earth observation data, offering access to multi-decadal imagery (40+ years), climatological records, and demographic datasets [37], [38]. Its scalable architecture enables robust data mining and visualization capabilities for scientific, governmental, and commercial applications. GEE's cloud processing infrastructure allows for fast and efficient computations, including automatic parallelization and caching of results to enhance efficiency [39]. The platform supports complex geospatial analyses via a JavaScript and Python API, offering rapid prototyping and visualization tools. It includes a browser-based IDE for using the Earth Engine JavaScript API. Access requires a Google Account with Earth Engine privileges. The IDE simplifies coding and data analysis, making it accessible to non-specialists and enabling quick algorithm development.

Additionally, GEE's easy accessibility and open access make it an invaluable resource for research, education, and government purposes. Its comprehensive API supports a range of geospatial analysis functions, such as image processing, classification, and time series analysis. The online code editor allows users to search for datasets, write and execute scripts, and manage assets seamlessly. With its combination of efficient computation, expansive data availability, and user-friendly interface, Google Earth Engine stands as a cornerstone in the field of geospatial data analysis. Therefore, in this study, GEE is used for tasks like processing and analyzing large datasets related to flood hazards (e.g., soil data, water, vegetation, wetlands, and historical flood maps). And extracted relevant geospatial information about buildings (e.g., location, elevation, land use) from satellite imagery or topographic data. More details about all layers are in the following section, 2.3.1

# **Analytic Hierarchy Process:**

Developed by Saaty (1970s) [40], the AHP provides a systematic framework for multi-criteria decision-making through hierarchical structuring of decision components (criteria, sub-criteria, and alternatives). This methodology employs pairwise comparisons to derive relative weights indicating parameter importance [41]. The results are synthesized to determine the best choice. AHP is particularly useful in geospatial applications for weighing and combining different data layers. Such as in this study, we use the layers (digital elevation models, DEM, soil properties, water, land use from buildings, vegetation, and wetlands) to create comprehensive flood index assessment maps. These multi-criteria are almost all data special to the Nile Delta region of Egypt, focusing on the resilience assessment of the buildings according to the literature review [26,28,30,32,34,42,43], where each study area has other different criteria according to the topography of the study area.

Additionally, AHP is widely used in risk mapping, especially for assessing the vulnerability of buildings and infrastructures. By incorporating various data layers such as terrain, proximity to water bodies, and historical flood data, AHP helps prioritize areas at higher risk and aids in strategic planning and emergency response [44]. Research has shown that AHP provides a systematic approach to evaluating multiple risk factors, leading to more robust land-use decision processes and disaster management [45–47].

Therefore, AHP offers several advantages over existing platforms. First, it allows for the systematic incorporation of expert opinions and subjective judgments, leading to more nuanced and comprehensive risk assessments [48]. Second, the process of pairwise comparisons enhances the consistency and reliability of the analysis [49]. Third, AHP is flexible and adaptable, allowing it to be applied to various geospatial and risk assessment scenarios [50]. So, mathematical equations are used to calculate weights and synthesize preferences [51]. For instance, the analysis constructs a pairwise comparison matrix quantifying inter-criteria relationships through numerical weights. Priority vectors are subsequently derived via eigenvector decomposition, while comparison consistency is verified through calculated consistency ratios (CR) using Eq 1:

$$CR = \frac{CI}{RI}$$
 Eq 1

The consistency ratio (CR), derived from the quotient of the consistency index (CI) (Eq 2 and 3) and random index (RI), the maximum eigenvalue  $\lambda max$  serves as a validation metric, with CR < 0.1 indicating acceptable judgment consistency. Reference values for RI appear in

Table 1.

$$CI = \frac{\lambda max - n}{n - 1}$$

$$\lambda max = \frac{\sum sum}{n}$$
Eq 2

Table 1 Consistency ratios (CR) are derived using tabulated random index (RI) values.

Matrix Size (N)	1.00	2.00	3.00	4.00	5.00	6.00	7.00	8.00	9.00	10.00
Random consistency index (RI)	0.00	0.00	0.55	0.89	1.11	1.25	1.35	1.40	1.45	1.49

### 2.3. The proposed framework

This section outlines the methodological framework for assessing the flood hazard index based on the spatial analysis subjected to static flood events. The proposed framework consists of many main stages, including.

The study employed a combined AHP-GIS approach. Consisting of four phases, including the conceptual framework of the GIS environment for this study area. (i) Identification and Preparation of Static Flood Hazard Parameters: Static flood hazard parameters were identified using GIS in the Nile Delta, Egypt, which experiences regular flooding of varying degrees. The sensitivity score of each parameter was assigned based on previous literature. (ii) Spatial Analysis and Flood Hazard Zone Estimation: Spatial analysis was conducted in the GIS environment to estimate flood hazard zones. Five relevant physical factors were selected for this analysis: elevation, soil permeability, slope, water bodies, and land use. (iii) AHP-based Factor Weighting: A pairwise comparison matrix was constructed to evaluate and quantify the relative contributions of each physical factor to flood susceptibility. The derived weights reflect each parameter's influence on hazard potential. (iv) FHI Computation: A GIS-integrated multi-criteria analysis framework was implemented, incorporating the weighted factors to calculate the comprehensive Flood Hazard Index.

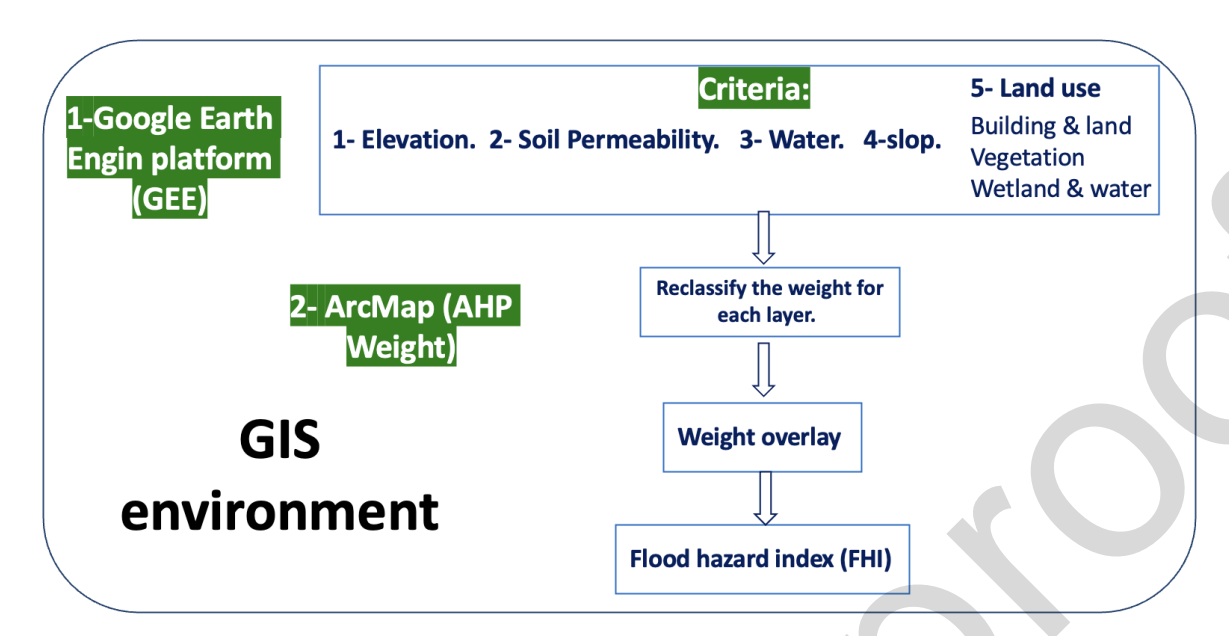


Fig. 2. Proposed an integrated framework for flood hazard index assessment.

# 2.3.1. Identification of Parameters in Exposure Modeling

This section details the flood hazard parameters employed to evaluate coastal community vulnerability to SLR impacts within Egypt's Nile Delta region.

#### **Elevation**

The primary criterion for the flood hazard index is elevation. The GMTED2010 global elevation model, developed by USGS, represents a significant advancement over previous datasets like GTOPO30 (30 arcsecond resolution). This new product offers seven enhanced raster datasets at resolutions of 30-, 15-, and 7.5-arcseconds, integrating the most accurate global topographic data available [52]. GMTED2010 primarily utilizes NGA's 1-arcsecond SRTM DTED® (<a href="https://science.jpl.nasa.gov/projects/srtm/">https://science.jpl.nasa.gov/projects/srtm/</a>) as its foundational dataset. To address data gaps in SRTM coverage, supplementary sources were incorporated, including: CDED, SPOT 5 Reference 3D, NED for North America, Australia's GEODATA 9-second DEM, and satellite-derived elevation models for Antarctica and Greenland. Our analysis specifically examines the Nile Delta DEM for elevations ranging from 0 to 1 meter above sea level, projected through 2100."

#### Soil Type

The second criterion is the subsurface Nile Delta soil type. It is the most important exposure criterion for the resilience index, which depends on the frequency of damage states of the building. While the satellite can't describe this deep layer. As noted by soil scientist Cristine Morgan, the current state of soil science knowledge lags behind space research, creating a significant knowledge gap given soil's critical role in sustaining terrestrial ecosystems. Soil texture classifications followed the USDA system, with characterization performed at six depth intervals (0-200 cm) at 250 m spatial resolution [53].

#### **Free-Flowing Water**

The third criterion is the free-flowing water to simulate the degree of saturation of the soil around the building. HydroSHEDS delivers standardized hydrographic data for multi-scale analyses through a comprehensive collection of geospatial datasets. The product includes vector and raster layers such as drainage networks, basin delineations, flow direction matrices, and cumulative flow calculations. River network representations are provided as polyline features, maintaining topological consistency across all HydroSHEDS products. The underlying raster data has a spatial resolution of 15 arc-seconds (~500 m equatorial ground resolution) [54].

# **Slope**

**The fourth criterion** is the slope of the Earth, which is used to simulate water flow directions. Slope gradients were derived by computing elevation differentials between each 30 m SRTM DEM pixel and its neighborhood mean, employing circular moving windows with radii of 115.8, 89.9, 35.5, 13.1, 5.6, 2.8, and 1.2 kilometers.

#### **Land Use**

**The fifth criterion** is land use. The ESA World Cover 2020 dataset offers 10-meter resolution global land cover classification derived from Sentinel-1 and Sentinel-2 satellite imagery. Developed under ESA's 5th Earth Observation Envelope Program (EOEP-5), this product categorizes surface features into 11 distinct classes [55].

# 3. RESULTS AND DISCUSSION

#### 3.1. Weighting and Pairwise Comparison

The AHP provides a systematic framework for multi-criteria decision analysis. It is widely used in risk mapping, especially for assessing the vulnerability of buildings and infrastructures [56]. AHP can help prioritize higher-risk areas and aid in strategic planning and emergency response [44]. AHP provides a systematic approach to evaluating multiple risk factors, leading to more informed DM in disaster management [45–47], [41]. AHP proves invaluable in geospatial contexts by evaluating and merging diverse data layers, exemplified in our study by incorporating DEM, soil characteristics, water bodies, land usage (including buildings), vegetation, and wetlands. These multi-criteria datasets are largely unique to the ND region in Egypt, concentrating on the assessment of building resilience [26,28,30,32,34,42,43]. After constructing a pairwise comparison matrix, the weights of each parameter are established based on their rank. A rating scale from 1 to 9 is used, with 1 indicating less importance and 9 indicating much higher importance.

**Table 2** displays the  $5\times5$  pairwise comparison matrix with unitary diagonal elements. where diagonal elements are equal to 1, where each study area has distinct criteria based on its topography. In this study, AHP is employed to determine the relative importance of these factors. Weight assignments were informed by both published literature and expert consultation (n=10 specialists in remote sensing and Delta region climate impacts). Following this evaluation, soil permeability received a relative importance score of 10 compared to slope, reflecting its greater influence in the analysis. Thus, the row has the inverse value of the pairwise comparison (e.g., 0.10 for soil permeability).

Table 2 Pairwise comparison matrix for static flood hazard.

Parameters	soil permeability	water	Elevation	land use	Slope
soil permeability	1.00	1.96	1.72	1.47	10.00
water	0.51	1.00	0.88	0.75	5.00
Elevation	0.58	1.14	1.00	0.86	6.67
Land use: 1-Vegetation.					
2-Building. 3-water.	0.68	1.33	1.16	1.00	6.67
4-land. 5-wetland.					
slope	0.10	0.20	0.15	0.15	1.00

Table 3 Parameter normalization using the AHP framework.

Parameters	Soil Permeability	Water	Elevation	Land use	Slope	Mean	$\mathbf{W_{i}}$
------------	-------------------	-------	-----------	----------	-------	------	------------------

Soil Permeability	0.348432	0.348226	0.351053	0.347284	0.340909	0.347181	3.471809
Water	0.177700	0.177595	0.178606	0.177559	0.170455	0.176383	1.763830
Elevation	0.202091	0.202458	0.203611	0.203580	0.227273	0.207803	2.078026
Land use	0.236934	0.236202	0.236189	0.236153	0.227273	0.234550	2.345500
Slope	0.034843	0.035519	0.030542	0.035423	0.034091	0.034084	0.340836

The normalized parameters undergo consistency validation through calculation of the consistency ratio (CR) using Eq 1, where RI = 1.11 (

$$\lambda max = \frac{\sum sum}{n}$$

Table 1) and  $\lambda_{\text{max}} = 5.01$  derived from Eq 2 the analysis maintains validity at the CR < 0.1 threshold.

Table 4 Parameter groupings and their assigned weight values.

Parameters	Class	Rating	Weights
- Tarameters	3 - 3 - 3 - 3 - 3 - 3 - 3 - 3 - 3 - 3 -		vicigitis
Soil Permeability	high (Sandy clay)	8	2 454000
Infiltration Level	medium (Silt)	6	3.471809
	low (Clay)	3	
Water	Permanent	9	1.763830
vv atei	non	0	1.703030
	0.00:+1.00 m	9	
	+1.00:+2.00 m	8	
Elevation	+2.00:+3.00 m	4	2.078026
	+3.00:+4.00 m	2	
	>+4.00 m	0	
Land use:	Urban	10	
1- Urban	Water	8	2.345500
2- Water	land	6	2.343300
3- Wetland	land	4	
4- Land 5- Vegetation	vegetation	2	
2 , egemion	constant	0	
	1	2	
Slope	2	4	0.340836
•	3	6	
	4	8	

The AHP assigned prioritized weights to six flood determinants (

Table 3). Soil permeability (SPIL) emerged as the most influential factor (weight = 3.48), reflecting its critical role in infiltration capacity and prolonged water retention. Elevation (2.07) and land use (2.34) followed, highlighting the vulnerability of low-lying urbanized areas. Water indices (1.76) and slope (0.34) exhibited lower but still significant contributions, consistent with the Delta's flat topography and dense hydrographic network. The CR < 0.1 validated the reliability of the pairwise comparisons.

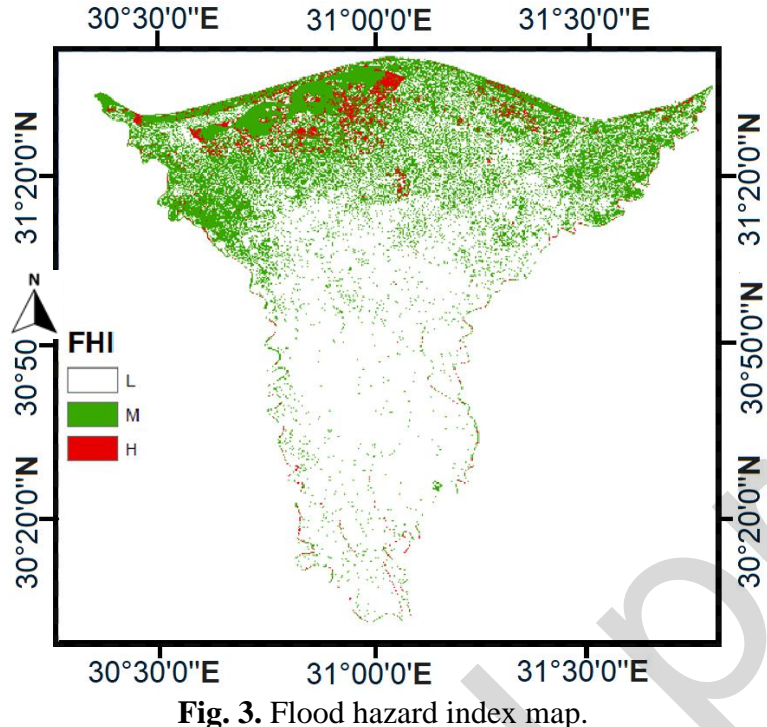
# 3.2. Flood Hazard Index Map

This section presents the spatial distribution of static flood hazard areas identified using the integrated GIS-AHP approach. The study area focuses on the Burullus Lake region within Kafr El-Sheikh Governorate, situated along the eastern Rosetta Nile branch in the northwestern Nile Delta **Fig. 3**. The flood hazard index map identifies high-risk static flood zones within this study area. The study area is confined between the Mediterranean Sea and Burullus Lake along a 40 km stretch parallel to Lake El-Burullus. Notably, approximately 11,000 buildings within this area are exposed to static flood hazards.

The integrated GIS-AHP model classified the study area into three distinct hazard levels Fig. 3. High-risk zones, covering 20% of the area, are primarily concentrated in the northwestern Delta, particularly in Kafr El-Sheikh Governorate along the eastern flank of the Rosetta Branch and the Burullus Lake shoreline. These areas exhibit elevations below 1 m, sand, well-draining soils, and proximity to water bodies. Moderate-risk zones, accounting for 35% of the study area, border high-risk regions and are characterized by 1–2 m elevations and mixed land use (agricultural and urban). The remaining 45% comprises low-risk zones, located further inland with elevations exceeding 2 m and clay-dominated soils with low permeability.

Burullus Lake, situated in northern Egypt's Kafr El-Sheikh Governorate, represents the largest natural lake in the country. This extensive body of brackish water covers an area of approximately 462 square kilometers. The Mediterranean Sea bounds the region along its northern periphery and agricultural zones to the south. A narrow sandbar with a width ranging from 600 meters to 5.5 kilometers separates the lake from the Mediterranean Sea. A 250-meter-wide and 10 cm to 5-meter-deep channel, known as the Burullus outlet, connects the lake to the sea.

The model's accuracy was assessed through cross-validation with historical coastal flood events (1972–2022), revealing an 85% spatial match between predicted high-risk zones and documented flood occurrences. Sensitivity analysis revealed that soil permeability was the most influential factor, accounting for 35% of the FHI variance, followed by elevation (20%) and water permanence (18%). Land use and slope collectively contributed the remaining 27%.



20 km

# CONCLUSIONS

This study has developed and implemented an innovative GIS-AHP framework to assess static flood hazards in Egypt's Nile Delta, yielding critical insights for flood risk management. Our integrated approach successfully identified and quantified five key physical determinants of flood vulnerability: (1) soil permeability (governing infiltration rates), (2) water presence (with permanent water bodies posing greater risk than temporary accumulations), (3) elevation (showing an inverse relationship with flood susceptibility), (4) land use patterns (particularly urban density), and (5) topographic slope (where flatter terrain exacerbates flood potential).

The northwestern Delta emerged as particularly vulnerable, with high-risk concentrations near Burullus Lake where low-lying topography, permeable soils, and proximity to water bodies converge. Our analysis revealed approximately 11,000 at-risk buildings in Kafr El-Sheikh Governorate alone. The GIS-AHP methodology not only provided systematic weighting of these factors through the FHI but also offers a transferable model for coastal flood assessment globally.

These findings carry significant implications for adaptive planning in deltaic regions facing sea-level rise. By precisely mapping hazard zones and quantifying contributing factors, this research provides a science-based foundation for targeted infrastructure protection, land-use regulations, and community resilience strategies in the Nile Delta and similar vulnerable coastal systems. The study underscores the urgent need to integrate such assessments into climate adaptation policies to safeguard both ecosystems and human settlements.

This study makes three significant advances in flood risk assessment for deltaic regions. First, it demonstrates the effectiveness of combining cloud-based GEE with AHP, providing a scalable solution that overcomes traditional data processing limitations in large-scale assessments. Second, the research delivers policy-ready outputs by precisely identifying vulnerable areas, particularly the critical more than 40 km coastal zone between Burullus Lake and the Mediterranean, enabling targeted protective measures and land-use planning. Most importantly, the work bridges disciplinary divides by innovatively integrating remote sensing data, hydrogeological factors, and socio-spatial variables - a combination that addresses the persistent gap in dynamic flood modeling for complex delta environments.

While this study provides valuable insights into flood risk assessment, several limitations should be acknowledged. The reliance on 30m SRTM DEM and 10m land-use data may obscure micro-topographic features critical for understanding local flood dynamics. Additionally, the use of static snapshots (e.g., Landsat 8 imagery) fails to capture important seasonal and episodic flooding patterns. Finally, human factors such as rapid population growth, unplanned urbanization, and adaptive infrastructure measures (e.g., seawalls) were not incorporated into the model, potentially influencing long-term risk trajectories. These constraints highlight opportunities for future refinements in both data collection and modeling approaches.

For future directions to enhance flood risk assessment in the Nile Delta, several research advancements should be pursued. First, higher-resolution modeling using LiDAR or UAV-derived DEMs (≤1m resolution) could significantly refine elevation-based risk evaluations. Second, integrating climate models (e.g., RCP scenarios) with subsidence data would enable dynamic projections of cumulative (SLR) impacts. Third, expanding the framework to incorporate socioeconomic factors such as population density, asset exposure, and adaptive capacity would support more holistic risk management strategies. Finally, leveraging AI techniques like convolutional neural networks (CNNs) for flood prediction could automate hazard classification and enhance real-time monitoring. This study highlights the urgent need for adaptive governance in the Nile Delta, where SLR poses escalating threats to communities and critical infrastructure. Moving forward, stakeholder engagement must be prioritized to translate risk maps into actionable policies, ensuring long-term resilience in a warming climate.

#### ACKNOWLEDGMENTS

We would like to express our deepest gratitude to our professors and advisors for their unwavering support, invaluable guidance, and insightful advice throughout this research. Their expertise and encouragement were instrumental in the completion of this work.

# REFERENCE

- [1] Teng J, Jakeman A J, Vaze J, Croke B F W, Dutta D and Kim S 2017 Flood inundation modelling: A review of methods, recent advances and uncertainty analysis Environmental modelling & software 90 201–16
- [2] Salman A M and Li Y 2018 Flood risk assessment, future trend modeling, and risk communication: a review of ongoing research Nat Hazards Rev **19** 04018011
- [3] Najafi M R, Zhang Y and Martyn N 2021 A flood risk assessment framework for interdependent infrastructure systems in coastal environments Sustain Cities Soc 64 102516
- [4] Masson-Delmotte V, Zhai P, Pirani A, Connors S L, Péan C, Berger S, Caud N, Chen Y, Goldfarb L and Gomis M I 2021 Climate change 2021: the physical science basis Contribution of working group I to the sixth assessment report of the intergovernmental panel on climate change 2
- [5] Golz S, Schinke R and Naumann T 2015 Assessing the effects of flood resilience technologies on building scale Urban Water J 12 30–43
- [6] Blanco-Vogt A and Schanze J 2014 Assessment of the physical flood susceptibility of buildings on a large scale—conceptual and methodological frameworks Natural Hazards and Earth System Sciences 14 2105–17
- [7] Hammond M J, Chen A S, Djordjević S, Butler D and Mark O 2015 Urban flood impact assessment: A state-of-the-art review Urban Water J 12 14–29
- [8] Blanc J, Hall J W, Roche N, Dawson R J, Cesses Y, Burton A and Kilsby C G 2012 Enhanced efficiency of pluvial flood risk estimation in urban areas using spatial-temporal rainfall simulations J Flood Risk Manag 5 143-52
- [9] Chen K-F and Leandro J 2019 A conceptual time-varying flood resilience index for urban areas: Munich city Water (Basel) 11 830

- [10] Peacock W G, Brody S D, Seitz W A, Merrell W J, Vedlitz A, Zahran S, Harriss R C and Stickney R 2010 Advancing resilience of coastal localities: Developing, implementing, and sustaining the use of coastal resilience indicators: A final report Hazard reduction and recovery center 1–148
- [11] Gornitz V 1991 Global coastal hazards from future sea level rise Palaeogeogr Palaeoclimatol Palaeoecol 89 379–98
- [12] Huang Y and Cheng H 2013 The impact of climate change on coastal geological disasters in southeastern China Natural hazards 65 377–90
- [13] Dasgupta S, Laplante B, Meisner C, Wheeler D and Yan J 2009 The impact of sea level rise on developing countries: A comparative analysis Clim Change **93** 379–88
- [14] Nicholls R J and Tol R S J 2006 Impacts and responses to sea-level rise: A global analysis of the SRES scenarios over the twenty-first century Philosophical Transactions of the Royal Society A: Mathematical, Physical and Engineering Sciences **364** 1073–95
- [15] Nicholls R J 2004 Coastal flooding and wetland loss in the 21st century: changes under the SRES climate and socio-economic scenarios Global Environmental Change 14 69–86
- [16] Nicholls R J 2002 Analysis of global impacts of sea-level rise: a case study of flooding Physics and Chemistry of the Earth, Parts A/B/C 27 1455–66
- [17] Nicholls R J, Hoozemans F M J and Marchand M 1999 Increasing flood risk and wetland losses due to global sea-level rise: regional and global analyses Global Environmental Change 9 S69–87
- [18] Xingong L, Rowley R J, Kostelnick J C, Braaten D, Meisel J and Hulbutta K 2009 GIS Analysis of Global Impacts from Sea Level Rise Photogramm Eng Remote Sensing **75** 807–18
- [19] Gravelle G and Mimura N 2008 Vulnerability assessment of sea-level rise in Viti Levu, Fiji Islands Sustain Sci 3 171–80
- [20] El-Nahry A H and Doluschitz R 2010 Climate change and its impacts on the coastal zone of the Nile Delta, Egypt Environ Earth Sci **59** 1497–506
- [21] Al-Jeneid S, Bahnassy M, Nasr S and El Raey M 2008 Vulnerability assessment and adaptation to the impacts of sea level rise on the Kingdom of Bahrain Mitig Adapt Strateg Glob Chang 13 87–104
- [22] Natesan U and Parthasarathy A 2010 The potential impacts of sea level rise along the coastal zone of Kanyakumari District in Tamilnadu, India J Coast Conserv 14 207–14
- [23] Marfai M A and King L 2008 Potential vulnerability implications of coastal inundation due to sea level rise for the coastal zone of Semarang city, Indonesia Environmental Geology **54** 1235–45
- [24] Kuleli T, Şenkal O and Erdem M 2009 National assessment of sea level rise using topographic and census data for Turkish coastal zone Environ Monit Assess **156** 425–34
- [25] UNDRR 2019 Global assessment report on disaster risk reduction United Nations Office for Disaster Risk Reduction (UNDRR)
- [26] Stanley J-D and Clemente P L 2017 Increased land subsidence and sea-level rise are submerging Egypt's Nile Delta coastal margin GSA Today 27 4–11
- [27] El-Raey M, Fouda Y and Nasr S 1997 GIS assessment of the vulnerability of the Rosetta area, Egypt to impacts of sea rise Environ Monit Assess 47 59–77
- [28] El-Marsafawy S, Bakr N, Elbana T and El-Ramady H 2019 The Soils of Egypt Climate ed H EL-Ramady, T Alshaal, N Bakr, T Elbana, E Mohamed and A-A Belal The Soils of Egypt 69–92
- [29] Anon NASA Google Earth
- [30] El-Saharty S, Nassar H, Shawky S, Elshalakani A, Hamza M M, Zhang Y and Zeltoun N 2022 Achieving the Demographic Dividend in the Arab Republic of Egypt: Choice, Not Destiny (World Bank Publications)
- [31] Hereher M E 2010 Vulnerability of the Nile Delta to sea level rise: an assessment using remote sensing Geomatics, Natural Hazards and Risk 1 315–21
- [32] Hemeda S 2021 Geotechnical modelling of the climate change impact on world heritage properties in Alexandria, Egypt Herit Sci 9 73

- [33] Elagouz M H, Abou-Shleel S M, Belal A A and El-Mohandes M A O 2020 Detection of land use/cover change in Egyptian Nile Delta using remote sensing The Egyptian Journal of Remote Sensing and Space Science 23 57– 62.
- [34] Shalaby A and Tateishi R 2007 Remote sensing and GIS for mapping and monitoring land cover and land-use changes in the Northwestern coastal zone of Egypt Applied Geography 27 28–41
- [35] Dawod G M, Ebaid H M, Haggag G G and Al-Karagy E M 2021 An Integrated Geomatics Approach for Projecting Sea Level Variations and Risks A Case Study in the Nile Delta, Egypt Journal of Architecture and Civil Engineering 6 15–29
- [36] Gebremichael E, Sultan M, Becker R, El Bastawesy M, Cherif O and Emil M 2018 Assessing Land Deformation and Sea Encroachment in the Nile Delta: A Radar Interferometric and Inundation Modeling Approach J Geophys Res Solid Earth 123 3208–24
- [37] Gorelick N, Hancher M, Dixon M, Ilyushchenko S, Thau D and Moore R 2017 Google Earth Engine: Planetary-scale geospatial analysis for everyone Remote Sens Environ **202** 18–27
- [38] Mutanga O and Kumar L 2019 Google Earth Engine Applications Remote Sensing 2019, Vol. 11, Page 591 11 591
- [39] Kumar L and Mutanga O 2018 Google Earth Engine applications since inception: Usage, trends, and potential Remote Sens (Basel) **10** 1509
- [40] Saaty T L 2004 Decision making the Analytic Hierarchy and Network Processes (AHP/ANP) Journal of Systems Science and Systems Engineering 2004 13:1 **13** 1–35
- [41] Saaty T L 2016 The analytic hierarchy and analytic network processes for the measurement of intangible criteria and for decision-making International Series in Operations Research and Management Science 233 363–419
- [42] Elbasiouny H and Elbehiry F 2019 Geology BT The Soils of Egypt ed H El-Ramady, T Alshaal, N Bakr, T Elbana, E Mohamed and A-A Belal 93–109
- [43] Belal A A, Mohamed E S and Abu-Hashim M S D 2015 Land evaluation based on GIS-spatial multi-criteria evaluation (SMCE) for agricultural development in dry Wadi, Eastern desert, Egypt International Journal of Soil Science 10 100–16
- [44] Ishizaka A 2019 Analytic Hierarchy Process and Its Extensions 81–93
- [45] Liu Y, Eckert C M and Earl C 2020 A review of fuzzy AHP methods for decision-making with subjective judgements Expert Syst Appl 161 113738
- [46] Munier N and Hontoria E 2021 Uses and Limitations of the AHP Method (Springer)
- [47] Arroyo P, Tommelein I D and Ballard G 2014 Comparing AHP and CBA as Decision Methods to Resolve the Choosing Problem in Detailed Design J Constr Eng Manag **141** 04014063
- [48] Alyami S H, Rezgui Y and Kwan A 2015 The development of sustainable assessment method for Saudi Arabia built environment: weighting system Sustain Sci 10 167–78
- [49] Aydiner C, Sen U, Koseoglu-Imer D Y and Can Dogan E 2016 Hierarchical prioritization of innovative treatment systems for sustainable dairy wastewater management J Clean Prod 112 4605–17
- [50] Calabrese A, Costa R, Levialdi N and Menichini T 2016 A fuzzy analytic hierarchy process method to support materiality assessment in sustainability reporting J Clean Prod 121 248–64
- [51] Dos Santos P H, Neves S M, Sant'Anna D O, Oliveira C H de and Carvalho H D 2019 The analytic hierarchy process supporting decision making for sustainable development: An overview of applications J Clean Prod 212 119–38
- [52] Danielson J J and Gesch D B 2011 Global multi-resolution terrain elevation data 2010 (GMTED2010)
- [53] Hengl T 2018 Soil texture classes (USDA system) for 6 soil depths (0, 10, 30, 60, 100 and 200 cm) at 250 m Zenodo, December 24
- [54] Grill G, Lehner B, Thieme M, Geenen B, Tickner D, Antonelli F, Babu S, Borrelli P, Cheng L and Crochetiere H 2019 Mapping the world's free-flowing rivers Nature 569 215–21

- [55] Zanaga D, Van De Kerchove R, De Keersmaecker W, Souverijns N, Brockmann C, Quast R, Wevers J, Grosu A, Paccini A, Vergnaud S, Cartus O, Santoro M, Fritz S, Georgieva I, Lesiv M, Carter S, Herold M, Li L, Tsendbazar N-E, Ramoino F and Arino O 2021 ESA WorldCover 10 m 2020 v100
- [56] Akkaya G, Turanollu B and Öztaş S 2015 An integrated fuzzy AHP and fuzzy MOORA approach to the problem of industrial engineering sector choosing Expert Syst Appl **42** 9565–73